Available online at www.sciencedirect.com

SciVerse ScienceDirect

Ceramics International 39 (2013) 6189–6197

CERAMICS INTERNATIONAL

www.elsevier.com/locate/ceramint

Thermal shock damage evaluation of refractory castables via hot elastic modulus measurements

A.P. Luz[a,*], T. Santos Jr.[a], J. Medeiros[b], V.C. Pandolfelli[a]

[a]Federal University of São Carlos (UFSCar), Materials Engineering Department, Rod. Washington Luiz, km 235, São Carlos, SP 13565-905, Brazil
[b]Petrobras, Research and Development Center (CENPES), Rio de Janeiro, RJ 21941-915, Brazil

Received 1 December 2012; received in revised form 7 January 2013; accepted 15 January 2013
Available online 21 January 2013

Abstract

When refractory castables are submitted to continuous thermal changes, crack nucleation and/or propagation can take place resulting in a loss of mechanical strength and overall degradation of such materials. This work evaluates the thermal shock damage cycling of high-alumina and mullite refractory castables designed for petrochemical application. Hot elastic modulus analyses were carried out after 0, 2, 4, 6, 8 and 10 thermal cycles ($\Delta T = 800$ °C) in order to investigate the microcracking evolution due to the temperature changes. Additionally, apparent porosity, hot modulus of rupture, erosion and work of fracture measurements were also performed. According to the attained results, it was detected at which temperature range the stiffening or embrittlement took place in the mullite-based refractory (M-SA) microstructure. Nevertheless, the damage induced by the thermal shock tests was not permanent, as further increase of the elastic modulus results was observed for all evaluated samples after annealing. On the other hand, the alumina-based composition containing a sintering additive (TA-SA) presented enhanced mechanical strength, high thermal stability and E values. Simulations indicated that refractories with high E values (~140 GPa, such as those attained for alumina-based castable) showed a reduced amount of stored elastic strain energy even under severe thermal stresses, which seems to be a key aspect for the engineered design of thermal shock resistance materials.
© 2013 Elsevier Ltd and Techna Group S.r.l. All rights reserved.

Keywords: C. Thermal shock; D. Mullite; Alumina; Hot elastic modulus

1. Introduction

Refractory castables are usually subjected to severe thermo-mechanical stresses, derived from an association of thermal shock, erosion, corrosion and mechanical impact [1–4]. The performance of such materials is temperature dependent and their response is affected by many factors (physical properties, phase transformations, reactions between the castables constituents, and others) which take place during firing and in service.

Assessing the refractory castable property degradation due to thermal stresses can be attained by quenching selected specimens out of a furnace at high temperatures into water, liquid metal, oil, fused salts or air [5–7]. This procedure leads to crack nucleation and/or propagation, spoiling the castables' mechanical strength. Additionally, as the crack formation has a major effect on the Young's modulus (E) of these materials, measuring such a property with the help of non-destructive techniques (sonic resonance, ultrasonic echography, transient vibration, internal friction and damping attained by resonance methods, etc.) may provide useful information to follow the progress of the thermal shock damage level [6,8–10].

In general, the engineering design of refractory castables for applications presenting marked temperature changes are mainly based on (1) the thermoelastic approach to evaluate the thermal stress level for fracture initiation, and (2) an energy balance concept to minimize thermal shock damage [11,12]. Furthermore, it is suggested that to attain the latter requirement, the castable could present crack initiation under severe service conditions, but limited amount of crack propagation [13,14]. These materials usually show lower brittleness, which

*Corresponding author. Tel.: +55 16 33518253; fax: +55 16 33615404.
E-mail addresses: anapaula.light@gmail.com (A.P. Luz), vicpando@ufscar.br (V.C. Pandolfelli).

0272-8842/$ - see front matter © 2013 Elsevier Ltd and Techna Group S.r.l. All rights reserved.
http://dx.doi.org/10.1016/j.ceramint.2013.01.038

can be a suitable requirement for many applications. It must be highlighted that the refractory materials brittleness can be defined by the ratio of the stored elastic strain energy at crack initiation and its work of fracture [14].

Some authors [13] also state that a decrease of brittleness is mainly attained by a reduction of strength and, therefore, stronger refractories should not be the best option. The fracture stress (σ_f) and the overall Young's modulus (E) (including the porosity) are properties that directly depend on the processing steps, after selecting the initial raw materials. Decreasing the refractory strength will result in a cascade negative effect on the elastic modulus and, consequently, affecting the thermal shock behavior.

High-alumina refractory castables are commonly used in risers for petrochemical fluid catalytic converters (FCC). In this kind of application, the working life of these materials will depend on their performance under temperature cycling and high speed particle erosion. However, although high-alumina castables attain the erosion resistance required, they do not usually show suitable densification and thermal shock behavior at temperatures close to 800 °C (FCC working condition). Calcium aluminate cement (CAC)-bonded compositions usually start their densification at temperatures above 1200 °C [15]. Therefore, to attain a high performance at temperatures where CAC does not show its optimized properties, sintering additives leading to liquid formation and, consequently, faster densification are an interesting technological alternative [16]. Nevertheless, selecting these additives should be tailored, as a liquid phase can result in refractoriness drawbacks.

As recently reported by Braulio et al. [16,17], due to the presence of a transient liquid phase derived from a boron-based compound (inducing densification without deteriorating the materials' high-temperature properties), remarkable hot mechanical properties for in situ spinel-forming and colloidal-bonded refractory castables could be attained.

Considering these aspects, the aim of this work is to evaluate the in situ thermal shock damage cycling of high-alumina and high-mullite refractory castables designed for petrochemical applications containing a boron-based sintering additive able to speed up the system densification at lower temperatures. Hot elastic modulus tests (using the bar resonance method) were carried out in order to follow the phase transformations and microcrack generation progress in dried samples (110 °C for 24 h) and after thermal shock cycling (0, 2, 4, 6, 8 and 10 with $\Delta T = 800$ °C). Furthermore, apparent porosity, hot modulus of rupture, erosion resistance and fracture energy measurements were also performed for a better understanding of the castables' behavior.

2. Experimental

High-alumina and high-mullite self-flowing castables were designed according to Alfred's packing model ($q = 0.21$) [18]. The compositions comprised coarse tabular alumina ($d \leq 6$ mm, Almatis, USA) or synthetic mullite (Mulcoa, Treibacher, Brazil) as aggregates, calcium aluminate cement (CAC, Secar 71, Kerneos, France) as a binder, reactive aluminas (CL370C and CT3000SG, Almatis, USA) and a boron-based additive ($d < 45$ μm, SA, under patent application) in order to speed up the densification of the refractories in the usual temperatures for petrochemical applications (~800 °C for FCC risers) [17]. Additionally, two sintering additive-free compositions (TA and M) were prepared and tested as reference materials.

Although previous works [19,20] investigated the use of high cement content (8–12 wt%) in refractory compositions for such application, the erosion resistance of those materials were rarely below 5 cm^3. Moreover, the addition of high amounts of CAC usually leads to other drawbacks during the first heat-up stage, as the steam (generated due to the dehydration of the cement phases) may become pressurized within the ceramic structure, occasionally causing cracking or even explosive disintegration of the products. Thus, as will be discussed in the following section of the present paper, the use of a sintering additive allows a possible decrease of the cement content without spoiling the mechanical strength and erosion resistance of the developed castables. Table 1 presents further details of the formulated castables, the water content added during the mixing step and the measured free-flow values.

Table 1
General information of the castables compositions.

	Compositions (wt%)			
	TA	**TA-SA**	**M**	**M-SA**
Raw materials				
Tabular alumina ($d \leq 6$ mm)	79.0	77.0	–	–
Mullite aggregates ($d \leq 3$ mm)	–	–	84.5	83.5
Reactive aluminas (CL370C and CT3000SG)	17.0	17.0	11.5	10.5
Calcium aluminate cement (Secar 71)	4.0	4.0	4.0	4.0
Sintering additive ($d \leq 45$ μm)	–	2.0	–	2.0
Properties				
Water content (wt%)	4.4	4.4	5.5	5.5
Free-flow (%)	72 ± 3	70 ± 2	64 ± 4	60 ± 3

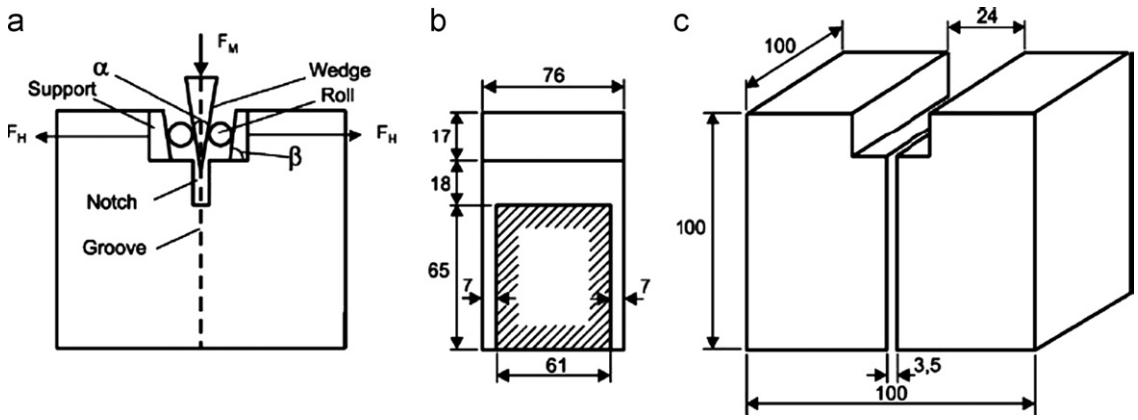

Fig. 1. (a) The test fixture and sample dimensions (all dimensions in mm) for the wedge splitting test, (b) cross-section of the sample, passing through notch and lateral grooves, and (c) the geometry and dimensions of the sample (all measures are presented in mm) [24].

The castable dispersion was carried out by adding 0.2 wt% of a polycarboxylate based dispersant (Basf, Germany). The compositions were dry-homogenized for 1 min and mixed for an additional 4 min in a rheometer specially developed for refractory castables, by adding the mixing water using a two-step procedure [21,22].

After the mixing step, prismatic samples (150 mm × 25 mm × 25 mm) were molded, cured at 50 °C for 24 h in a humid environment (relative humidity = 80%) and dried at 110 °C for 24 h, followed by firing at 600, 800, 1000 and 1200 °C for 5 h in an electrical furnace (Lindberg Blue, Lindberg Corporation, USA). Hot modulus of rupture (HMOR) tests were carried out at 600 °C, 800 °C, 1000 °C and 1200 °C (using samples pre-fired at the same testing temperature) in HBTS 422 equipment (3-point bending test, Netzsch, Germany) based on the ASTM C583–8 standard. The erosion resistance measurements of pre-fired castable samples (800 °C for 5 h) were also performed, following the ASTM C704 standard (1 kg of no. 36 grit silicon carbide to erode samples 10 cm × 10 cm × 2.5 cm thick, leading to a weight loss that was converted to a volumetric one).

Concerning the thermal shock tests, pre-fired refractories (800 °C for 5 h) were subjected to a total of 10 heating and cooling cycles (ASTM C1171–91). The samples were placed into a furnace chamber previously heated at 825 °C and kept at this temperature for 15 min. After that, they were withdrawn and cooled in air for another 15 min, leading to thermal gradients of roughly 800 °C. This procedure was considered as one full cycle. The damage caused by the thermal changes was evaluated by the elastic modulus measurements at room temperature (bar resonance, ASTM C 1198–91) as a function of the thermal cycles (0, 2, 4, 6, 8 and 10).

In order to perform in situ analysis of the microstructural transformations and the thermal shock damage cycling, hot elastic modulus tests were carried out in the prismatic samples after previous processing steps (curing at 50 °C for 24 h and drying at 110 °C for 24 h, and after pre-firing at 800 °C/5 h and subjected to 0, 2, 4, 6, 8 and 10 thermal cycles). The bar resonance method (which is based on sample excitation and detecting the correspondent vibration spectrum using piezoelectric transducers [23]) was also used in such analyses. The measurements were conducted in the 30–1000 °C range with a heating rate of 2 °C min^{-1}.

The apparent porosity of the samples attained after 0, 2, 4, 6, 8 and 10 thermal cycles was measured by the Archimedes method (ASTM C380–00), using kerosene as the immersion liquid. Due to its enhanced performance in the thermal shock experiments, TA-SA pre-fired samples (800 °C/5 h, samples dimension as presented in Fig. 1) with a notch and lateral grooves along the crack propagation plane were also prepared for wedge splitting tests [24]. In order to carry out the stable crack propagation measurements, the castable was placed in an appropriate holder together with the device containing the supports, the rollers and the wedge (wedge angle = 10°).

This set was adapted on MTS equipment (MTS 810), where the experiments were performed using a 50 kN load cell and crack opening displacement (COD device) at a constant speed (i.e., the rate was fixed at 0.01 mm min^{-1}). The fracture energy values (γ_{wof}) were attained by the following equation:

$$\gamma_{wof} = \frac{1}{2A}\int P_M d\delta \quad (1)$$

where, A is the projected area of the fracture surface, P_M is the vertical load applied by the testing machine, and δ is the displacement of the machine's actuator. The value of the integral $\int P_M d\delta$is determined by the total area under the corresponding load-displacement curve.

3. Results and discussion

3.1. Thermo-mechanical and thermal shock damage cycling evaluation

Fig. 2 shows the hot modulus of rupture (HMOR) and the eroded volume of the designed castable samples. Lower

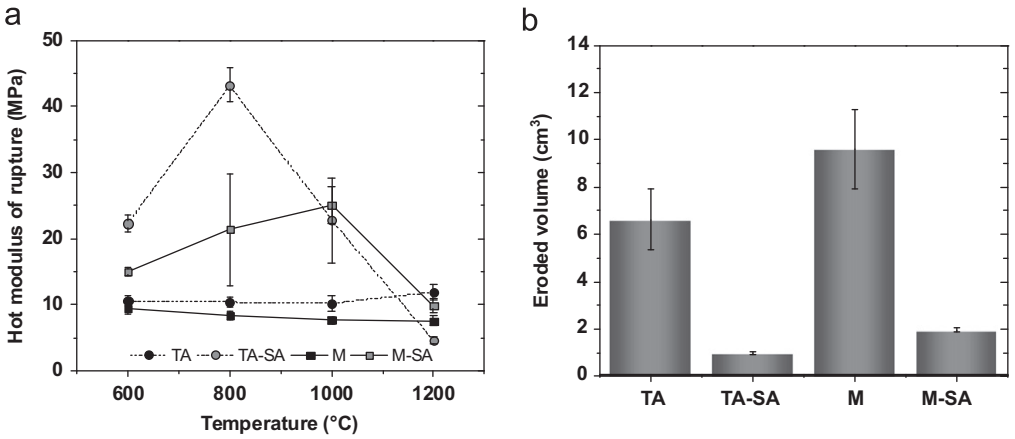

Fig. 2. (a) Hot modulus of rupture (HMOR) for samples pre-fired for 5 h at the same testing temperature (600, 800, 1000 or 1200 °C) and (b) eroded volume for samples pre-fired at 800 °C for 5 h.

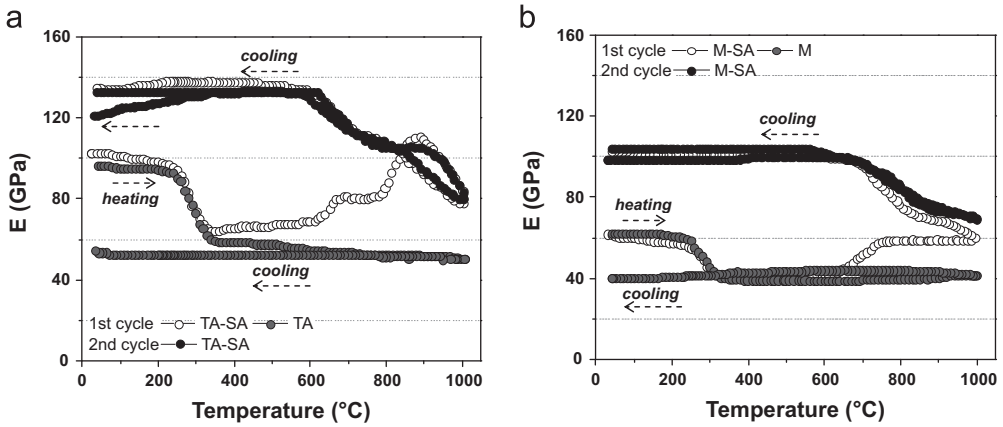

Fig. 3. *In situ* elastic modulus evolution as a function of the temperature (heating and cooling cycles up to 1000 °C): (a) for alumina-based compositions, with or without sintering additive (SA), and (b) for mullite-based castables, with and without sintering additive (SA). The evaluated samples were previously cured at 50 °C for 24 h and dried at 110 °C for another 24 h.

mechanical strength values were observed for castables TA and M (additive-free compositions, Fig. 2a) mainly between 600–1000 °C, which is the temperature range where the cement hydrates have already been decomposed [25]. HMOR increase only took place at 1200 °C for TA samples, where calcium aluminate phases were formed (CA and CA_2, C= CaO and $A=Al_2O_3$. X ray diffraction [XRD] profiles, confirming the presence of such components in the selected sample, are not shown here). Castable M, on the other hand, showed roughly the same mechanical strength results at 1000 and 1200 °C (7.6 MPa). This feature highlights the late densification of these compositions, pointing out that plain CAC is not the most suitable binder system for low temperature applications of both high-alumina and mullite refractory castables.

By adding the sintering additive to the cement-containing castables, the densification was anticipated and TA-SA and M-SA showed their maximum HMOR values at 800 °C and 1000 °C, respectively. Considering that the FCC risers working condition is close to 800 °C, the designed castables presented excellent mechanical strength for this application which was reflected in the very low erosion values attained (Fig. 2b). Nevertheless, it was also observed that when increasing the testing temperatures above 1000 °C, the hot mechanical strength rapidly decreased as a consequence of liquid formation (Fig. 2a).

Aiming to evaluate the densification effect induced by the sintering additive, *in situ* E analyses up to 1000 °C were carried out for dried samples. Fig. 3 presents the elastic modulus results attained during the first thermal cycle for the four designed castables. Additionally, for the TA-SA and M-SA samples, a second heating cycle was also performed.

The alumina-based compositions (TA and TA-SA) presented higher E values (96–102 GPa) after drying at 110 °C when compared to the mullite ones (M and M-SA, 61–62 GPa). All compositions featured a characteristic decrease of the elastic modulus in the 200–400 °C temperature range (1st heating cycle) due to the cement-hydrates decomposition [25]. Moreover, no major changes in the E results betwen 400–1000 °C and during cooling

were detected for the TA and M castables, indicating that no densification and further microstructural transformations took place.

Conversely, castable TA-SA presented an E increase between 600–900 °C, pointing out the sample's sintering and densification. Above 900 °C, the elastic modulus decreased due to the formation of liquid that started reducing the castable hot mechanical properties. This E drop is due to the remaining liquid in the composition, as no dwell time at 1000 °C was carried out in this test. Later, it will be shown that this liquid crystallizes for holding times higher than 5 h at 800 °C. While cooling, the TA-SA elastic modulus presented a marked increase up to roughly a constant value (~137 GPa), which is related to the material's stiffening [26]. For the second heating cycle in the same sintering additive containing sample (TA-SA), the E values showed a similar profile to the first one. However, the cooling cycle was slightly different mainly below 350 °C, as the thermal expansion mismatch of the present phases resulted in microcracks and a final elastic modulus value (121 GPa) lower than the initial one at room temperature (137 GPa).

For the mullite-based composition containing the sintering additive (M-SA, Fig. 3b), the elastic modulus increased in the 600–750 °C range (1st heating cycle), mainly due to the sample densification process induced by the SA reactions with the castable's components (mullite, alumina and calcia). While cooling, the M-SA elastic modulus also presented a major increase (~103 GPa) and, during the second thermal cycle, this sample kept its enhanced performance presenting some E changes only in the 600–1000 °C temperature range due to the structure softening.

Based on the final elastic modulus results after two thermal cycle measurements (Fig. 3), castable TA-SA showed higher E values (121 GPa) than the M-SA composition (~103 GPa). The high mechanical performance attained for the TA-SA samples at 800 °C (Fig. 2a) led to a concern regarding its thermal shock behavior, as strong materials, in general, result in catastrophic thermal shock failures owing to their ability to store high elastic energy. However, TA-SA pre-fired samples (800 °C/5 h) showed a very high initial elastic modulus (~137 ± 7 GPa) and, more relevant than that, almost no decrease in the elastic modulus as a function of the number of thermal cycles (0–10 cycles, Fig. 4). When compared to the additive-free composition (TA), a major difference was observed and the measured E values for samples TA were 2.5 fold lower than the TA-SA ones after two or more cycles. Such a distinct performance reinforces the importance of the selected sintering additive.

The mullite-based castables, on the other hand, showed high initial elastic modulus (M-SA = 97 ± 3 GPa) and almost no E change for the M composition after two thermal cycles (Fig. 4). Additionally, no significant difference between the M and M-SA samples results after 10 cycles was observed. In order to better understand the TA-SA and M-SA behavior, additional *in situ* elastic modulus analyses were carried out for samples pre-fired at 800 °C for 5 h and submitted to 0, 2, 4, 6, 8 and 10 thermal shock cycles. Fig. 5 shows the E curves as a function of the temperature for the selected compositions.

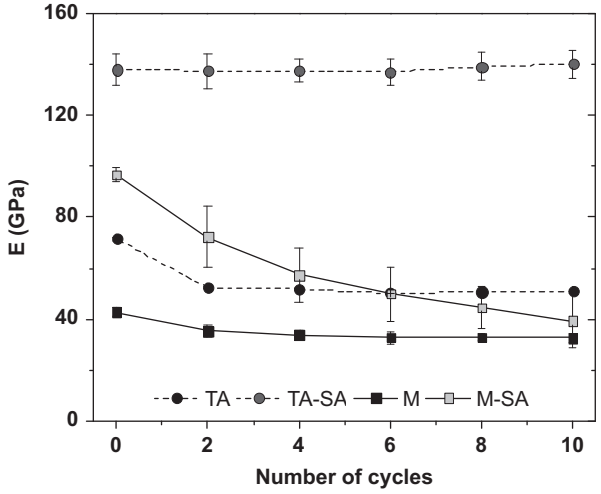

Fig. 4. Elastic modulus of the castable samples (pre-fired at 800 °C/5 h) after thermal shock cycling tests (ΔT = 800 °C).

Again castable TA-SA showed higher thermal stability, as the elastic modulus values were kept in the range of 108–127 GPa, resulting in the superposition of the attained curves (Fig. 5a). After pre-firing the TA-SA samples at 800 °C for 5 h, the liquid phase previously identified in this composition during their first heating cycle (Fig. 3a) was consumed, giving rise to $Al_4B_2O_9$, $Al_{18}B_4O_{33}$ and $CaAl_2B_2O_7$ phases (according to additional XRD tests) and, consequently, inhibiting further E decay. The same trend was not observed for the mullite-based castable (M-SA) and a significant decrease of the initial E values after each analyzed cycle was detected. Based on Fig. 5b, some general features can also be highlighted:

(1) *from 30 up to 700 °C:* the E increase after the thermal shock should be related to the crack closing effect.
(2) *from 700 °C up to 800 °C:* the presence of a low amount of liquid phase mainly affected the performance of the M-SA samples analyzed after 0 and 2 cycles (E decrease) in this temperature range. Nevertheless, no deterioration of the castables' thermal properties is expected to take place at the working conditions of the FCC equipments, as high HMOR values were attained at 800 °C and 1000 °C (Fig. 2).
(3) *from 800 °C down to 580 °C:* during the first step of the cooling cycle, an increase in the elastic modulus was observed for the thermal shocked samples. This E variation is related to the usual stiffening of the material when the temperature drops due to the increase in the liquid phase viscosity.
(4) *from 580 °C down to room temperature:* the decay of E values after 2 quenching cycles is associated with the development of flaws (i.e., opening of the cracks

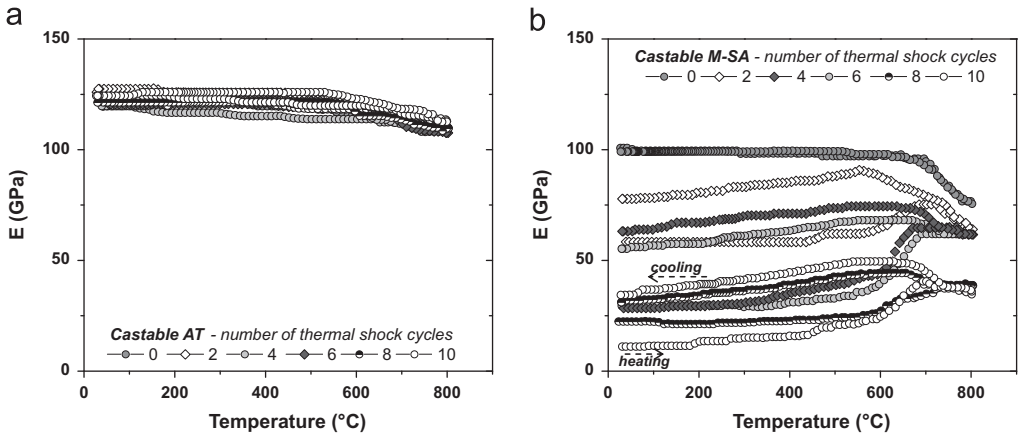

Fig. 5. In situ elastic modulus evaluation up to 800 °C (heating and cooling cycles) for: (a) TA-SA and (b) M-SA samples attained after different thermal shock cycles. Both castables were pre-fired at 800 °C for 5 h.

Table 2
Initial and final E values results attained after the evaluated thermal cycles (ΔT=800 °C) for the M-SA castable.

Cycles	$E_{initial}$ (GPa)	E_{final} (GPa)	Percentual elastic modulus variation (%)
0	101	99	−2
2	58	78	+34
4	30	55	+110
6	28	63	+96
8	22	31	+41
10	11	34	+209

partially closed during the beginning of the heating cycle or new crack formation) induced by the thermal expansion mismatch among the phases comprising the castable' samples. Nevertheless, an important aspect to be pointed out is that the damage caused by the temperature changes were not permanent, as a further increase of the elastic modulus results (due to crack healing and other mechanisms) could be observed for those samples ($E_{final} > E_{initial}$, as shown in Table 2). Considering the E evolution as a function of the thermal cycles, it can be observed that the M-SA thermal cycling damage is reduced after a heating cycle (annealing effect).

Regarding the apparent porosity results as a function of the thermal cycles, no statistical change in the pore volume content (%) was observed for the TA-SA and M-SA samples (Fig. 6a) between the 2nd and 10th thermal cycle. According to the model proposed by Rossi [27] to predict the elastic modulus behavior of composites materials, this property can be extensively influenced by the shape of pores/flaws or inclusions contained in the final microstructure. Rossi stated that depending on the c/a ratio (where a is the spheroidal radius of the flaw/inclusion and c is the major axis parallel to the stress vector) a marked E decrease can be detected even for low porosity content changes (i.e., c/a=0.01 curve, Fig. 6b).

Hence, crack coalescence (leading to changes in the shape and length of the flaws) might be the main factor responsible for the reduction of the M-SA samples' elastic modulus initial values after 2, 4, 6, 8 and 10 thermal shock cycles, although the porosity has barely changed.

Based on the attained results, one important question still remains "how can the TA-SA refractory (with high E and σ_f) present such a remarkable thermal shock resistance?". In order to answer this question, some extra thermo-mechanical and fracture energy measurements, as well as simulations of the stored elastic strain energy $\left(\frac{1}{2}\frac{\sigma_f^2}{E}\right)$ behavior in the castable samples were carried out.

3.2. Additional evaluation of the TA-SA castable samples

Some additional samples were prepared, pre-fired at 800 °C for 5 h and submitted to HMOR (at 200, 400, 600 and 800 °C) and wedge splitting tests for a better understanding of its mechanical behavior at lower temperatures and to estimate the fracture surface energy necessary for the material's failure, respectively. Fig. 7a shows that TA-SA castable showed an outstanding performance (43–48 MPa) between 200–800 °C. HMOR values were sixfold higher than the vibratable castable currently used in Brazilian FCC units (43 vs 7 MPa at 800 °C). The difference between the results shown in Fig. 2a and Fig. 7a is that for the

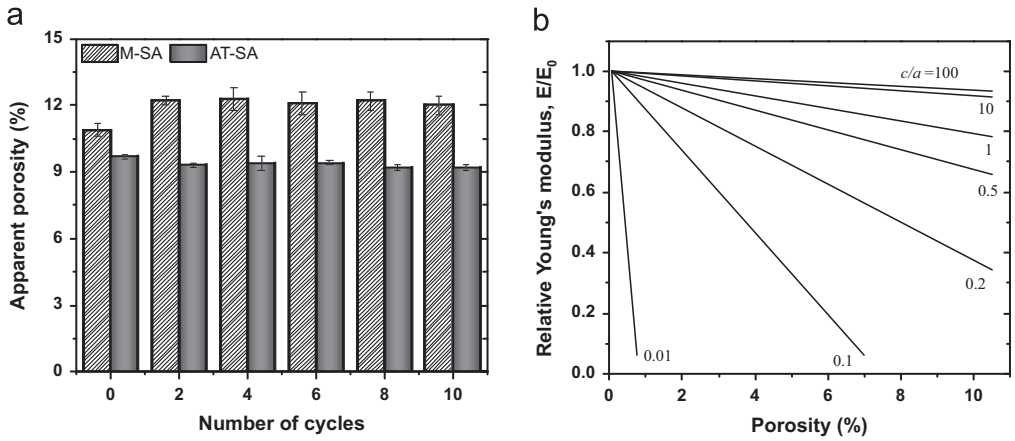

Fig. 6. (a) Apparent porosity results of the castable samples attained after the thermal shock experiments ($\Delta T \sim 800$ °C), and (b) effect of oriented spheroidal cavities/pores on the relative Young's modulus of a composite material [27].

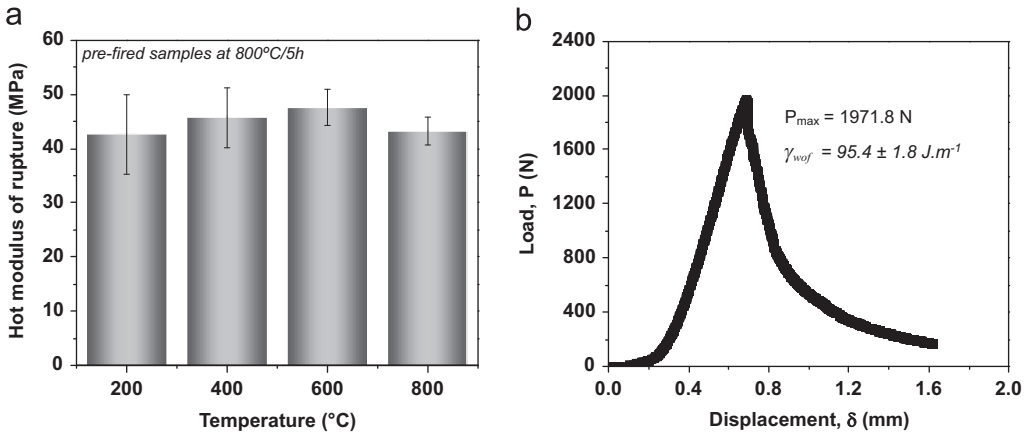

Fig. 7. (a) Hot modulus of rupture as a function of temperature and (b) load versus displacement curve attained in the wedge splitting test for the pre-fired TA-SA samples (firing temperature = 800 °C/5 h).

former, the samples were fired for 5 h at the testing temperatures (600–1200 °C), whereas for the latter, they were all pre-treated at 800 °C/5 h and tested at 200, 400, 600 and 800 °C.

Moreover, based on the load-displacement curve (Fig. 7b) and the further analysis of the samples fractured surface, the good cohesion of the castable matrix, the strong matrix-aggregate bond and the transgranular crack propagation were evident, although the fracture energy ($\gamma_{wof} = 95.4 \pm 1.8$ J m^{-1}) value was not as high as expected. The crack propagation within the grains (transgranular fracture) usually leads to low thermal shock resistance due to its limited contribution to the fracture energy and the absence of crack deflection [24]. However, it is believed that the strong matrix-aggregate bond in the TA-SA samples resulted in high E levels, which could be an important characteristic to enhance the thermal stability of this refractory.

The simulation of the elastic strain stored energy $\left(\frac{1}{2}\frac{\sigma_f^2}{E}\right)$ in the castable samples as a function of E and σ_f (Fig. 8) indicated that refractory materials presenting low Young's modulus (i.e., 20 GPa) should store high elastic energy levels in their structure, especially when they are submitted to high thermal stress ($\sigma > 20$ MPa). Therefore, if the crack initiation is not avoided, then most likely the material failure should take place, as a significant amount of elastic energy must be dissipated. On the other hand, refractories with high E values ($\sim$140 GPa, as castable TA-SA) display low elastic strain energy value even under severe stresses ($\sigma \sim 50$ MPa, Fig. 8), which seems to be a key aspect for the engineered design of thermal shock resistance materials. Thus, although the literature states that stronger refractories (presenting high mechanical strength) are not always suitable, it can be assumed that they might be good options, as long as they present very high E values and if erosion resistance is an additional requirement.

4. Conclusions

The use of a sintering additive to speed up the refractory densification at lower temperatures seems to be a suitable

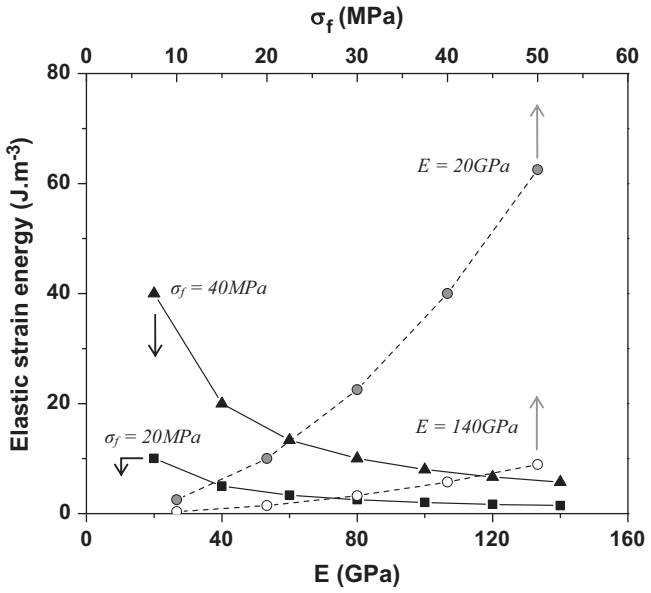

Fig. 8. Estimation of the elastic strain energy stored in the samples at crack initiation, considering constant values of σ_f (20 MPa) or E (20 and 140 GPa).

alternative to develop novel compositions for the FCC petrochemical units. The mullite castable composition (M-SA) showed interesting behavior under thermal shock cycling, as the damage induced by the temperature changes was not permanent and a further increase of the elastic modulus results could be observed ($E_{final} > E_{initial}$) after "annealing". Crack nucleation and coalescence seemed to be the main factor for the embrittlement of these samples. Conversely, the evaluated high-alumina-based castable (TA-SA) showed remarkable mechanical strength, thermal stability and high E values. Based on the calculated results of the elastic strain stored energy in the castable samples, it can be assumed that stronger refractories (with high mechanical strength) can be good options to be applied in environments presenting sudden temperature changes, as long as the material presents very high E values.

Furthermore, as presented in this work, the combined use of thermal shock experiments and hot elastic modulus measurements can be an important procedure to assess the thermo-mechanical performance of complex refractory castable compositions, pointing out the critical temperature range where such materials would be more susceptible to flaw generation and mechanical degradation.

Acknowledgments

The authors would like to thank FIPAI, CNPq and Petrobras for supporting this work. The help of Dr. T.M. Souza in the hot elastic modulus analyses is also appreciated.

References

[1] M. Ghassemi Kakroudi, E. Yeugo-Fogaing, M. Huger, C. Gault, T. Chotard, Influence of the thermal history on the mechanical properties of two alumina based castables, Journal of the European Ceramic Society 29 (2009) 3197–3204.
[2] N.M. Rendtorff, L.B. Garrido, E.F. Aglietti, Thermal shock and fatigue of zircon–mullite composite materials, Ceramics International 37 (2011) 1427–1434.
[3] V. Roungos, C.G. Aneziris, Improved thermal shock performance of Al_2O_3–C refractories due to nanoscaled additives, Ceramics International 38 (2012) 919–927.
[4] C. Aksel, Mechanical properties and thermal shock behavior of alumina–mullite–zirconia and alumina–mullite refractory materials by slip casting, Ceramics International 29 (2003) 311–316.
[5] B. Cotterel, W.O Sze, Q. Caidong, Thermal shock and size effects in castable refractories, Journal of the American Ceramic Society 78 (1995) 2056–2064.
[6] F. Damhof, W.A.M. Brekelmans, M.G.D. Geers, Experimental analysis of the evolution of thermal shock damage using transit time measurement of ultrasonic waves, Journal of the European Ceramic Society 29 (2009) 1309–1322.
[7] S. Marenovic, M. Dimitrijevic, T. Volkov Husovic, B. Matovic, Thermal shock damage characterization of refractory composites, Ceramics International 34 (2008) 1925–1929.
[8] J.M. Auvray, C. Gault, M. Huger, Microstructural changes and evolutions of elastic properties versus temperature of alumina and alumina–magnesia refractory castables, Journal of the European Ceramic Society 28 (2008) 1953–1960.
[9] R. Grasset-Bourdel, A. Alzina, M. Huger, D. Gruber, H. Harmuth, T. Chotard, Influence of thermal damage occurrence at microstructural scale on the thermochemical behaviour of magnesia-spinel refractories, Journal of the European Ceramic Society 32 (2012) 989–999.
[10] D.N. Boccaccini, M. Romagnoli, E. Kamseu, P. Veronesi, C. Leonelli, G.C. Pellacani, Determination of thermal shock resistance in refractory materials by ultrasonic pulse velocity measurement, Journal of the European Ceramic Society 27 (2007) 1859–1863.
[11] J. Homeny, R.C. Bradt, Thermal Shock of Refractories. Thermal Stresses in Material and Structures in Severe Thermal Environments, New York: Plenum Publishing Company, USA, 1980 343-363.
[12] V.R. Salvini, V.C. Pandolfelli, R.C. Bradt, Extension of Hasselman's thermal shock theory for crack/microstructure interactions in refractories, Ceramics International 38 (2012) 5369–5375.
[13] H. Harmuth, R.C. Bradt, Investigation of refractory brittleness by fracture mechanical and fractographic methods, Refractories Manual (2010) 6–10.
[14] H. Harmuth, E.K. Tschegg, A fracture mechanics approach for the development of refractory materials with reduced brittleness, Fatigue and Fracture of Engineering Materials and Structures 20 (11) (1997) 1585–1603.
[15] W.E. Lee, W. Vieira, S. Zhang, A. Ghanbari, H. Sarpoolaky, C. Parr, Castable refractory concretes, International Materials Reviews 46 (3) (2001) 145–167.
[16] M.A.L. Braulio, G.G. Morbioli, V.C. Pandolfelli, Advanced boron-containing Al_2O_3–MgO refractory castables, Journal of the American Ceramic Society 94 (2011) 3467–3472.
[17] M.A.L. Braulio, G.G. Morbioli, J. Medeiros, J.B. Gallo, V.C. Pandolfelli, Nano-bonded wide temperature range designed refractory castables, Journal of the American Ceramic Society 95 (2012) 1100–1104.
[18] R.G. Pileggi, F.T. Ramal Jr., A.E.M. Paiva, V.C. Pandolfelli, High performance refractory castables: particle size design, Refractory Applications and News 8 (2003) 17–21.
[19] S.F. Rahman, Advances in vibration—cast refractories for application as abrasion resistant linings, in: Proceedings of UNITECR'89, 1989, 955–965.
[20] R. Rothrock, L.P. Kreitz, New development in high strength, abrasion resistant castable, Ceramic Transactions: Advances in Refractory Technology 4 (1988) 272–293.
[21] R.G. Pileggi, V.C. Pandolfelli, A.E.M. Paiva, J. Gallo, Novel rheometer for refractory castables, American Ceramic Society Bulletin 79 (2000) 54–58.

[22] R.G. Pileggi, A. Studart, V.C. Pandolfelli, J. Gallo, How mixing affects the rheology of refractory castables–part I, American Ceramic Society Bulletin 80 (2001) 27–31.
[23] G. Pickett, Equations for computing elastic constants from flexural and torsional resonant frequencies of vibration of prisms and cylinders, Proceedings American Society for Testing Materials 45 (1945) 846–865.
[24] S. Ribeiro, J.A. Rodrigues, The influence of microstructure on the maximum load and fracture energy of refractory castables, Ceramics International 36 (2010) 263–274.
[25] A.P. Luz, V.C. Pandolfelli, Halting the calcium aluminate cement hydration process, Ceramics International 37 (2011) 3789–3793.
[26] A.P. Luz, M. Huger, V.C. Pandolfelli, Hot elastic modulus of Al_2O_3–SiC–SiO_2–C castables, Ceramics International 37 (2011) 2334–2345.
[27] R.C. Rossi, Prediction of the elastic moduli of composites, Journal of the American Ceramic Society 51 (1968) 433–439.